Optimized, unequal pulse spacing in multiple echo sequences improves refocusing in magnetic resonance

Elizabeth R. Jenista, Ashley M. Stokes, Rosa Tamara Branca, and Warren S. Warren[a)]
Department of Chemistry and Center for Molecular and Biomolecular Imaging, Duke University, North Carolina 27708-0346, USA

(Received 22 July 2009; accepted 22 October 2009; published online 30 November 2009)

A recent quantum computing paper (G. S. Uhrig, Phys. Rev. Lett. **98**, 100504 (2007)) analytically derived optimal pulse spacings for a multiple spin echo sequence designed to remove decoherence in a two-level system coupled to a bath. The spacings in what has been called a "Uhrig dynamic decoupling (UDD) sequence" differ dramatically from the conventional, equal pulse spacing of a Carr–Purcell–Meiboom–Gill (CPMG) multiple spin echo sequence. The UDD sequence was derived for a model that is unrelated to magnetic resonance, but was recently shown theoretically to be more general. Here we show that the UDD sequence has theoretical advantages for magnetic resonance imaging of structured materials such as tissue, where diffusion in compartmentalized and microstructured environments leads to fluctuating fields on a range of different time scales. We also show experimentally, both in excised tissue and in a live mouse tumor model, that optimal UDD sequences produce different T_2-weighted contrast than do CPMG sequences with the same number of pulses and total delay, with substantial enhancements in most regions. This permits improved characterization of low-frequency spectral density functions in a wide range of applications.
 [doi:10.1063/1.3263196]

I. INTRODUCTION

Quantum computing—the manipulation of a quantum mechanical system to do information processing—has attracted considerable attention since the mid-1990s, largely triggered by Shor's proposed algorithm for finding prime factors in polynomial instead of exponential time.[1] One of the earliest proposed implementations was solution phase NMR (Ref. 2) due to the long coherence times (leading to readily resolved resonances) and simple spin Hamiltonian. Despite theoretical objections that solution NMR quantum computers could never be scalable to a useful number of "qubits,"[3] this field saw substantial experimental research efforts aimed at developing implementations of quantum computing algorithms, with the high water mark probably being the demonstration that a seven-spin system could be made to factor the number 15.[4] In more recent years, experimental interest has largely shifted to systems such as trapped ions and quantum dots that, in principle, might be scalable. However, the theoretical framework has led to new insights into the nature of coherence, correlation, and entanglement, and to new ways to think about pulse sequences.

Here we present what might be the first case of this framework enabling magnetic resonance (MR) applications—in this case, extending the coherence lifetime (or, in the language of that community, reducing decoherence) in magnetic resonance imaging (MRI) of structured media. We start from a recently published result[5] that predicted a specific, optimal, highly *nonuniform* spacing for multiple echo sequences could significantly improve echo refocusing under certain models for relaxation. This set of timings is now commonly cited in the quantum computing community as the "Uhrig dynamic decoupling" or UDD sequence, and should be contrasted with the equal spacings used in virtually all MR experiments for over 50 years.[6,7] Recently, such lifetime extension has been experimentally demonstrated with the UDD sequence for ground state electron spin transitions of Be^+ atoms in a Penning trap[8] (with some caveats, as we discuss later). However, the phonon-mediated relaxation model was not directly relevant to MRI, and to our knowledge no such application has been suggested in any previous paper.

Here we show experimentally that this predicted spacing can significantly reduce MR transverse relaxation in the limit normally encountered in structured samples, and that it thus increases the signal in these images. Experimentally, this increase is not uniform; theoretically, it is expected to depend explicitly on the structure of the spectral density of the resonance frequency fluctuations, and therefore can be used to both characterize those fluctuations and improve contrast. Our demonstration experiments are in tissue (both *in vitro* and *in vivo*) but extensions to other applications involving relaxation measurements under restricted diffusion (such as confined gases in nanopores,[9] anisotropy in tissue,[10] director fluctuations in liquid crystals,[11] pore structure in rocks,[12] and molecular composition in trabecular bone[13]) or multiple pulse echo imaging in highly inhomogeneous fields[14] would be promising. We also connect this work to the standard framework for understanding MR multiple pulse sequences (average Hamiltonian theory) in order to lay the groundwork for understanding effects of rf inhomogeneity, nonzero pulse duration, and resonance offset effects.

[a)]Author to whom correspondence should be addressed. Tel.: (919)660-1508. FAX: (919)287-2454. Electronic mail: warren.warren@duke.edu.

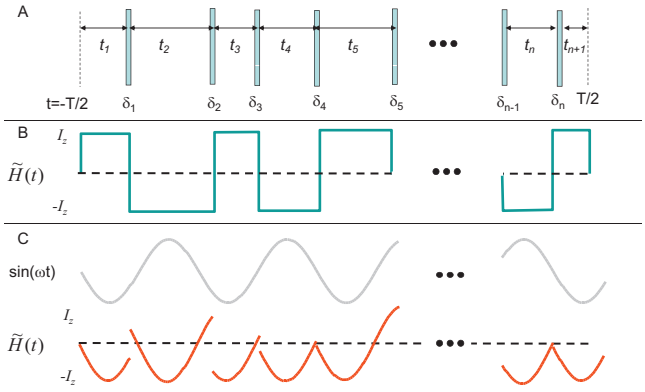

FIG. 1. (a) Generic multiple echo sequence. All pulses are π pulses with the same phase; the position of the ith pulse is δ_i and the delay just before the ith pulse is t_i. (b) Static resonance frequency variations are rotated by the π pulses, giving a toggling frame Hamiltonian $\tilde{H}$ proportional to $\pm I_z$ [in this case, $\tilde{H}$ is proportional to the modulation function $y(t)$]. As long as $t_1+t_3+t_5,\ldots=t_2+t_4+t_6,\ldots$, the effect cancels since $\tilde{H}$ averages to zero. (c) A time-varying frequency fluctuation ($\sin(\omega t)$) is altered by the pulse sequence but in general, $\tilde{H}$ is not averaged to zero even though $y(t)$ is unchanged. The UDD sequence in Fig. 2 does the best possible job of canceling extremely low-frequency fluctuations.

II. THEORY OF RELAXATION DURING MULTIPLE SPIN ECHO SEQUENCES

For the simplest ensembles of two-level systems, such as those found in solution NMR, the distinction between a "homogeneous" T_2 and "inhomogeneous" T_2^* lifetime is easy to make: Local variations in the magnetic field can be treated as a constant over the time between pulses, giving a static contribution to the spin Hamiltonian of the form $H=\hbar\Delta\omega(\vec{r})I_z$. In this limit (ignoring all pulse imperfections for the moment), a simple spin echo gives the same signal as a multiple echo sequence [Fig. 1(a)] of the same total length. Such multiple echo sequences are traditionally viewed in an interaction representation where the π pulses rotate the Hamiltonian instead of the initial magnetization, thus creating what is called a "toggling frame Hamiltonian"[15] $\tilde{H}$. In this case, $\tilde{H}$ changes sign after each π pulse,

$$\tilde{H}=\begin{cases}\hbar\Delta\omega(\vec{r})I_z & \text{during } t_1,t_3,t_5,\ldots\\ -\hbar\Delta\omega(\vec{r})I_z & \text{during } t_2,t_4,t_6,\ldots\end{cases}$$
$$\equiv\hbar\Delta\omega(\vec{r})y(t)I_z, \quad \text{where} \tag{1}$$
$$y(t)=\begin{cases}1 & \text{during } t_1,t_3,t_5,\ldots\\ -1 & \text{during } t_2,t_4,t_6,\ldots.\end{cases}$$

In Eq. (1) we follow the notation of Ref. 8 by introducing $y(t)$, the modulation of the Hamiltonian created by the pulses [which is also the function graphed in Fig. 1(b)]. The only spin operators ever present are $\pm I_z$, which makes it trivial to calculate the effects of the pulse sequence. As long as the sum of the even delays is equal to the sum of the odd delays, the average of $S(t)$ is zero, and the effect of resonance offset is removed [Fig. 1(b)]. In conventional notation,[15] the "average Hamiltonian" $\bar{H}=\int\tilde{H}(t)dt=0$.

Making $y(t)$ average to zero imposes only a single constraint on the delays, while leaving many degrees of freedom

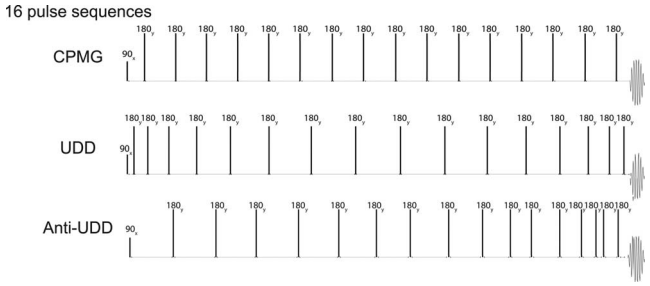

FIG. 2. 16-pulse CPMG, UDD, and anti-UDD pulse sequences. For example, for an 80 ms total echo time, the CPMG sequence has a uniform delay between the π pulses of 2.5 ms, except for the first and last delays, which are 1.25 ms each. The delays in the UDD sequence are 0.681, 2.02, 3.2902, 4.4483, 5.455, 6.2759, 6.883, 7.2558, 7.3814, 7.2558, 6.883, 6.2759, 5.455, 4.4483, 3.2902, 2.02, and. 681 ms. The anti-UDD sequence (see text) is a control sequence with the same delays as the UDD sequence, arranged in different orders.

to optimize them. For example, diffusion in a constant magnetic field gradient imposes an additional decay ($\exp(-\alpha t^3)$) on the magnetization.[6,16] It is then trivial to show that for a fixed total echo time and number of pulses, the best positioning is the Carr–Purcell–Meiboom–Gill[6,7] (CPMG) sequence shown in Fig. 2(a): equal delays T/n between the $n\pi$ pulses and delays of $T/2n$ before the first and after the last π pulses if n is even, or all delays equal to $T/(n+1)$ if n is odd. Some refinements have been made to CPMG experiments over the decades since they were introduced (including the introduction of composite[17] or shaped adiabatic pulses,[18] or of crusher gradients around each π pulse), but the basic structure of equal pulse spacing has remained uncontested.

In recent years, experiments have shown that in tissue, a 10–100 ms CPMG sequence often gives a higher signal intensity than does a spin echo sequence of the same total duration even without an externally applied gradient.[18] This arises from at least two effects. Susceptibility variations within even the smallest image voxels combine with diffusion to generate magnetic field fluctuations; in addition, magnetization transfer and migration between different compartments modulate the resonance frequency. Both of these effects create a time- and position-dependent resonance offset $\Delta\omega(\vec{r},t)$ with spectral density over a range of frequencies. The instantaneous phase shift $\phi(T)$ experienced during free evolution over an interval T is the time integral of this function, which in turn can be decomposed into its frequency components,

$$\phi(T)=\int_0^T\Delta\omega(\vec{r},t)dt=\int_{t=0}^{T}\int_{\omega=-\infty}^{\infty}G(\vec{r},\omega)e^{-i\omega t}d\omega dt. \tag{2}$$

[In what follows for simplicity we will drop the explicit position dependence, thus writing $\Delta\omega(t)$ or $G(\omega)$.].From Eq. (2) different groups of spins accumulate different extra random phase shifts, and the echo disappears; in practice, spin echo relaxation times of water in tissue at high fields can be a factor of 100 or shorter than in a test tube.

This is not the same physical model as motion in a constant gradient, but it remains intuitively reasonable to avoid long delays between pulses, hence CPMG would seem to be

the best choice. Remarkably, a recent theoretical quantum computing paper[5] shows that this is not, in general, correct. That paper showed that under specific circumstances, the optimum timing for $n\pi$ pulses is not the equidistant one; in our notation (centering the sequence at $t=0$), the jth pulse should be located at time

$$\delta_j = T\{\sin^2(\pi j/(2n+2)) - 0.5\}. \tag{3}$$

These timings are illustrated in Fig. 2(b) for the 16-pulse version. The sequence is symmetric with longer delays near the center. While the relaxation model in that paper is not directly relevant to MR, the simplicity of the results led to speculation[19] and later proof[20] that this was a universal result for a broad class of models of relaxation in two-level systems. This work has also been extended theoretically[21] to more complex, concatenated pulse sequences.

These papers are written with notation and language which are inconsistent and unfamiliar to the MR community. Here we rephrase their results, adapt them to the average Hamiltonian formulation, and slightly alter the model to make it more appropriate for MR. Consider a single frequency component in Eq. (2), $\hbar G(\omega)e^{i\omega t}I_z$. A multiple echo sequence will create a toggling frame Hamiltonian and (exact) average Hamiltonian of

$$\tilde{H} = \hbar G(\omega)y(t)e^{-i\omega t}I_z,$$
$$\bar{H} = \int \hbar G(\omega)y(t)e^{-i\omega t}I_z dt = \hbar G(\omega)\tilde{y}(\omega)I_z. \tag{4}$$

Figure 1(c) shows how $\tilde{H}$ is modulated, starting with a single sine wave component. Even if the sine wave itself were to go through an integral number of cycles during the pulse sequence, the average $\bar{H}$ would not generally be zero. Thus, a multiple echo sequence converts resonance frequency fluctuations at frequency ω into an average frequency shift that depends on the phase of the sine wave. Since $G(\omega)$ is expected to vary in phase across the sample, this causes position-dependent frequency shifts and signal dephasing proportional to $\int_{\omega=-\infty}^{\infty}|G(\omega)|^2|\tilde{y}(\omega)|^2 d\omega$. The quantity $|G(\omega)|^2$ as defined here is equivalent to the spectral density $J(\omega)$ in conventional NMR relaxation theory [or $S_\beta(\omega)$ in Ref. 8]; the quantity $|\tilde{y}(\omega)|^2$, which is in words just the power spectrum of the modulation function created by the pulses, is the function $F(\omega\tau)/\omega^2$ in Ref. 8.

Changing the delays in a multiple echo sequence changes $y(t)$ and $|\tilde{y}(\omega)|^2$, but Parseval's theorem shows that

$$\int_{-\infty}^{\infty}|\tilde{y}(\omega)|^2 d\omega \propto \int_{-T/2}^{T/2}|y(t)|^2 dt = \int_{-T/2}^{T/2}(1)dt = T. \tag{5}$$

Thus, if the resonance frequency fluctuations were uniform in frequency, changing the delays makes no difference at all—any multiple pulse echo sequence [or no pulses at all, $S(t)=1$] would perform exactly the same. However, since spin echoes do produce refocusing in tissue and CPMG sequences with $T \approx 10-100$ ms produce additional refocusing, we can infer that low-frequency components (relative to $1/T$) play an important role in the relaxation dynamics. This is also physically reasonable—for example, apparent diffusion coefficients in water correspond to motion over cellular distances (and hence exposure to susceptibility differences) in tens of milliseconds.

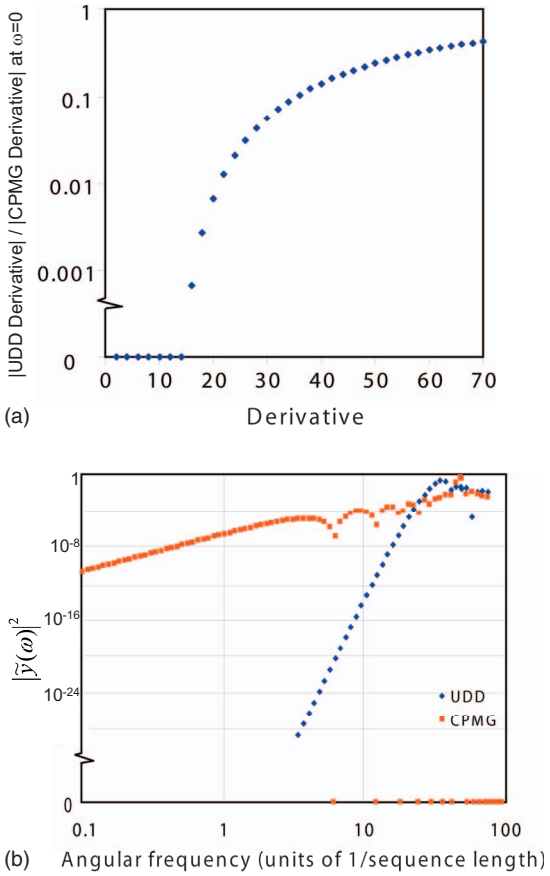

FIG. 3. (a) The pulse spacing in an n-pulse UDD sequence suppresses the effects of resonance frequency fluctuations at low frequency, making the first $(n-1)$ derivatives around $\omega=0$ vanish. This figure compares the even derivatives of the 16-pulse version to a CPMG sequence (which has a nonvanishing second derivative). Odd derivatives vanish for both. (b) Explicit comparison of the efficiency of frequency fluctuations (for example, from diffusion in a structured sample with susceptibility differences) in causing dephasing. This is proportional to the power spectrum of the modulation function created by the pulse train. This figure compares a 16-pulse UDD sequence and a 16-pulse CPMG sequence of the same duration. Note that for low-frequency modulation, UDD vastly outperforms CPMG in inhibiting relaxation.

As noted above, CPMG or any other sequence with $t_1+t_3+t_5,\ldots=t_2+t_4+t_6,\ldots$ makes the average value of $y(t)$ $(=\tilde{y}(\omega=0))$ vanish, and thus refocuses static resonance frequency variations. For any sequence symmetric about $t=0$ (including CPMG with an even number of pulses), all odd derivatives of $\tilde{y}(\omega)$ vanish at the origin. The key result of Ref. 5 is that the specific pulse placements in the n-pulse UDD sequence make all of the first $(n-1)$ derivatives $d^m\tilde{y}(\omega)/d\omega^m$ vanish at $\omega=0$. Equivalently, the first error term signal scales as the $(n+1)$ power of the sequence length. Thus, the suppression of relaxation effects at moderately low frequencies is optimally effective.

Figure 3 shows explicit calculations for a 16-pulse UDD sequence illustrating this point. Figure 3(a) shows that the first 15 derivatives at the origin vanish for the UDD sequence; for CPMG, even the second derivative is nonzero.

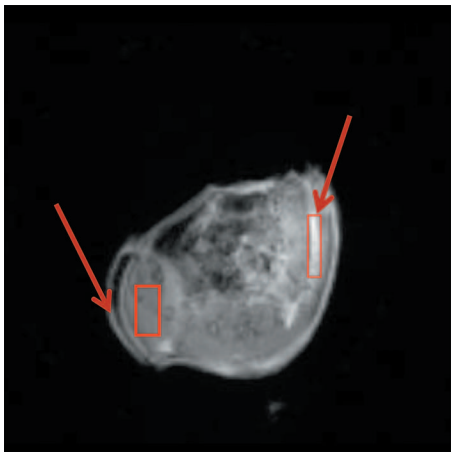

FIG. 4. Spin echo image of the postmortem mouse used in the experiments in Fig. 5. Arrows indicate locations in the mouse where there is excess free water since the mouse was frozen and thawed. The boxes in red show the ROIs used for the analysis of signal strength in Table I.

The consequence of this suppression for different frequencies is shown in Fig. 3(b). For almost all frequencies up to $\omega=25/T$, $\tilde{y}(\omega)$ is smaller for UDD than for CPMG and hence those frequencies are less effective in dephasing. Incidentally, the zeroes on the graph for CPMG at $\omega=2\pi/T$, $4\pi/T,\ldots$ are because of the periodic structure, but $\omega=16\pi/T$ is very large: At that frequency, $\tilde{y}(\omega)$ goes through a π phase shift during the delay between the pulses, and the sine wave is effectively rectified.

Reference 21 suggests that there would be applications to "high-precision NMR where narrow linewidths are a prerequisite," but this would appear to be unpromising. Multiple spin echo sequences remove or distort scalar couplings, and in any event the linewidth improvements are likely to be miniscule as resonance frequency fluctuations on the relevant time scale (seconds) are very small in an unstructured sample. However, T_2 extension is of great value in a variety of tissue imaging applications. For example, the most common intermolecular multiple-quantum coherence (iMQC) signals grow linearly with time,[22] and in most such applications, the maximum signal strength is directly proportional to T_2. Pairs of hyperpolarized spins can be prepared in the "singlet state" $\alpha\beta-\beta\alpha$ to increase their lifetime,[23,24] but if the two spins are inequivalent, multiple echo sequences (or removal from the magnet) are needed to prevent interconversion to $\alpha\beta+\beta\alpha$.[23] Even equivalent spins[24] might see a lifetime extension. More generally, different tissue microstructures would generate different resonance frequency fluctuations $G(\omega)$ that would not be expected to respond identically to the UDD sequence, so it could provide a new source of contrast reflecting subvoxel information that is not equivalent to any other existing sequences.

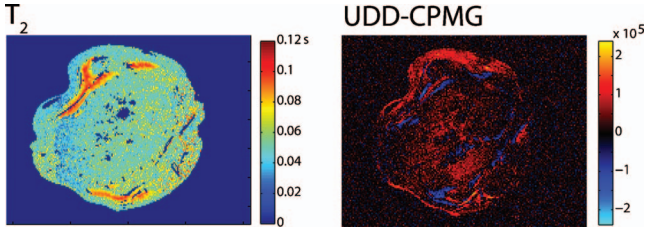

FIG. 6. Left: T_2 map on a postmortem mouse (different from the one in Figs. 4 and 5) obtained by fitting spin echo data from 10 to 160 ms. Right: difference image between eight-pulse UDD and eight-pulse CPMG (sequence length 80 ms). Regions with moderate T_2 benefit more from the UDD sequence than do the long T_2 regions.

III. EXPERIMENTAL METHODS

To test the hypothesis that UDD sequences provide additional refocusing, we compared imaging sequences on a postmortem mouse (Figs. 4–6) and *in vivo* in a tumor bearing mouse (Fig. 7). The mouse was placed in a supine position, and axial slices through the abdomen or through the tumor were selected. MRI data were acquired on a Bruker 7.05 T (^{1}H:300.5 MHz). In all cases we compared the contrast from three sequences: UDD, CPMG, and an "anti-UDD" sequence [Fig. 2(c)] with the same total delay and number of pulses, hence the same dissipated power. Pulse positions for the UDD sequences were calculated using

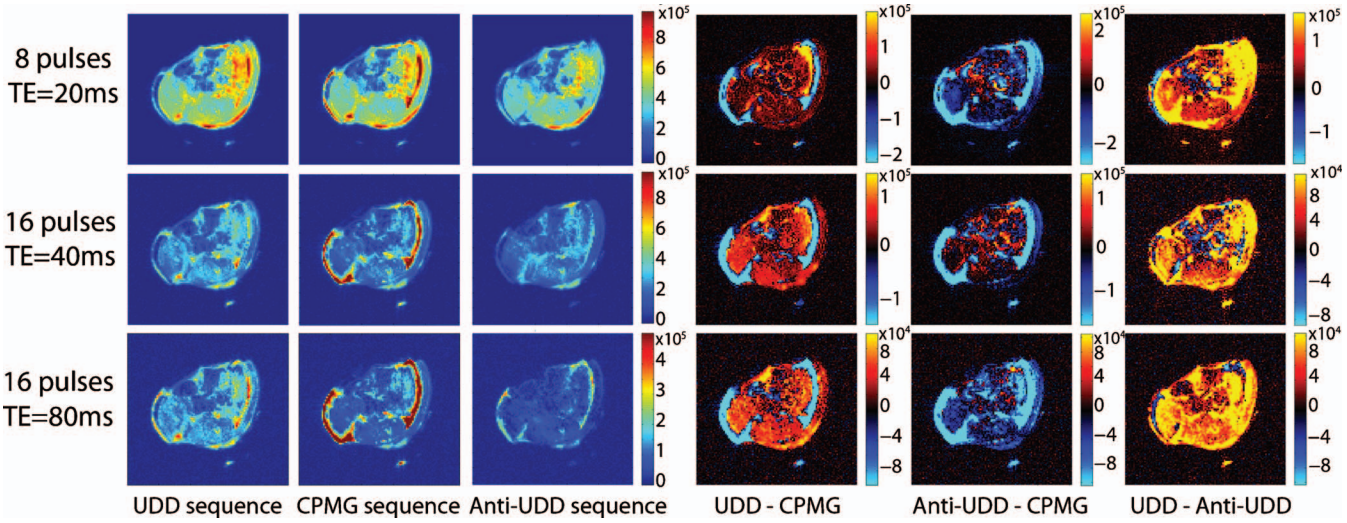

FIG. 5. Comparison of the UDD, CPMG, and anti-UDD pulse sequences on the postmortem mouse in Fig. 4. The effect of the UDD sequence is most apparent at the longer echo times, with larger numbers of pulses.

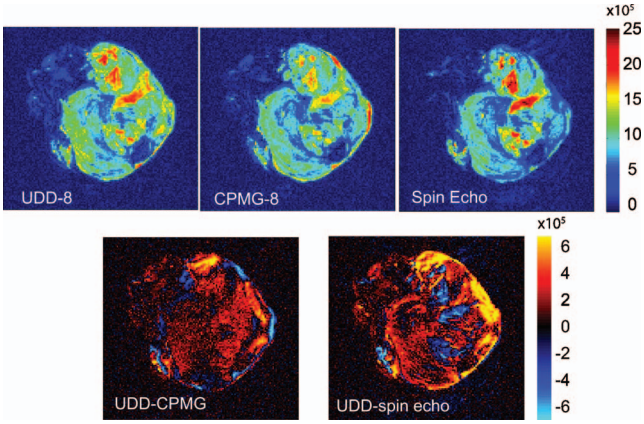

FIG. 7. *In vivo* axial images of tumor tissue obtained with eight-pulse UDD and CPMG sequences and with a spin echo sequence (120 ms total echo time). The tumor tissue appears highly inhomogeneous with several necrotic areas with a higher signal intensity. Differences between UDD, CPMG, and spin echo are typically ±25%.

TABLE I. Comparison of the signal strength from the UDD, anti-UDD, and CPMG sequences. Free water and tissue ROIs were selected, as shown in Fig. 4. Note that at the longer echo times with 16 pulses, the CPMG sequence refocuses the free water very well, while the UDD sequence has significantly improved signal-to-noise ratio in the tissue ROI. In addition, the anti-UDD sequence significantly underperforms both the UDD and CPMG sequence in the tissue ROI for the 16-pulse sequence with TE =80 ms.

	Free water	Tissue
UDD/CPMG, 8 pulse, TE=20 ms	1.03	1.41
Anti-UDD/CPMG, 8 pulse, TE=20 ms	0.69	1.35
UDD/Anti-UDD, 8 pulse, TE=20 ms	1.50	1.05
UDD/CPMG 16 pulse, TE=40 ms	0.40	1.22
Anti-UDD/CPMG 16 pulse, TE=40 ms	0.27	0.93
UDD/Anti-UDD, 16 pulse, TE=40 ms	1.50	1.31
UDD/CPMG, 16 pulse, TE=80 ms	0.52	1.71
Anti-UDD/CPMG, 16 pulse, TE=80 ms	0.32	0.59
UDD/Anti-UDD, 16 pulse, TE=80 ms	1.65	2.88

Eq. (3). The anti-UDD sequence was done as a control experiment. This sequence has exactly the same set of delays as UDD, and it still has $\tilde{y}(\omega=0)=0$ (e.g., $t_1+t_3+t_5,\ldots=t_2+t_4+t_6,\ldots$) so the echo timing is correct; however, the intervals are rearranged to set the longer delays upfront, and the shorter delays toward the end of the sequence. This will make even the first derivative $d\tilde{y}(\omega)/d\omega\neq 0$, and by the arguments above should make the refocusing performance worse.

For the postmortem experiments in Figs. 4 and 5, 2 and 1.267 ms Hermite pulses were used for excitation and refocusing, respectively. No phase cycling was performed and the images were all acquired without averaging. The echo time was varied between 40 and 80 ms. An 8 mm axial slice was then selected through the abdomen with a 8 cm field of view and a 256×256 matrix size. All the π pulses in each sequence were flanked by crusher gradients, and in our experience it is crucial to arrange crusher gradients in different directions (as discussed later).

For the comparison with a T_2 map (Fig. 6) and the *in vivo* experiment (Fig. 7), 0.5 ms Hermite pulses were chosen for both excitation and the eight refocusing pulses. A 2 mm axial slice was selected across the tumor. The total echo time for the spin echo, CPMG, and UDD was chosen equal to 120 ms for the *in vivo* experiment, 100 ms for the T_2 map, with a total of 8π pulses for CPMG and UDD. Other imaging parameters were 2 s repetition rate and 3 cm field of view. All images were processed using IMAGEJ (NIH, Bethesda, MD) and MATLAB software (Mathworks, Inc.).

IV. RESULTS AND DISCUSSION

Figures 4 and 5 compare CPMG, UDD, and anti-UDD sequences for a postmortem mouse that had recently been thawed (giving a significant amount of free water, indicated by the arrows). In general, the CPMG sequence highlights the free water deposits in the subcutaneous layers, the UDD sequence highlights the tissue architecture, and the anti-UDD sequence gives overall weaker signals. Differences are much more evident with more pulses (which increases the number of zeroed derivatives in the UDD sequence) and with longer echo times (which reduces the effects of duty cycle).

In most cases, the UDD sequence provides more signal in bulk tissue than both the CPMG and anti-UDD sequences (Fig. 5, signal comparisons in Table I). In particular, the difference images in Fig. 5 show that that the UDD sequence provides better refocusing of the tissue signal, and the anti-UDD sequence does not have as much signal in bulk tissue as the CPMG or UDD sequence; for the long echo time (80 ms) sequence with 16 pulses, the UDD:CPMG:anti-UDD signal ratios are 1.7:1:0.34 in the indicated tissue region of interest (ROI). However, the improvement provided by UDD is not just a uniform factor, and in fact the free water refocuses better with CPMG. Since the local structure is different in those regions, differences are to be expected. Figure 6 provides a direct comparison (different sample from Figs. 4 and 5) of a T_2 map with an image of the difference between UDD and CPMG; from the figure it is clear that on average, regions with moderately short T_2 show better UDD signals than do the longest T_2 regions, but it is also clear that there is no simple relation between T_2 and UDD-CPMG. This implies the contrast in the latter image is not simply equivalent to what could have been inferred from simple T_2 weighting.

Figure 7 shows an *in vivo* application on a nude mouse bearing a human prostate tumor (the bright regions, showing a longer T_2 value, correspond to the necrotic area of the tumor, whose size exceeds 4 cm^3). A trend similar to the postmortem experiment was seen in this *in vivo* study: Most of the bulk tissue gives more signal with the UDD sequence, but the bright regions with free water do not. Understanding these trends (or indeed, proving them to be universal) will require significant additional studies; however, since the UDD sequence serves as a very sharp high-pass filter for frequency fluctuations, careful variation of the overall sequence length could provide a very effective mapping method for $J(\omega)$, and could reasonably be expected to provide a wealth of structural information that is not accessible by conventional MR methods.

The analysis presented here so far has been idealized (as has the discussion in the quantum computing literature), and

thus it is critical to verify that our signal differences are not just artifacts from pulse sequence imperfections. A quantitative comparison of expected signal intensity between, for example, a spin echo and a CPMG sequence requires careful attention to pulse flip angles, effects of diffusion during crusher gradients, effects of finite pulse length, and dephasing effects due to scalar couplings in the nonwater components of the tissue. However, comparisons between UDD, CPMG, and anti-UDD sequences (which is the measure used here) are much easier to quantify. In general, all of these effects are readily handled by the average Hamiltonian theory, and have been handled in many different contexts over the years.[15] The most important consequence of rf inhomogeneity for CPMG sequences is stimulated echoes,[25] where some of the signal arises from magnetization which was stored along the z axis for part of the sequence. Experimentally, we find that with as few as four pulses and the homogeneity from a normal body imaging coil ($\sim \pm 5\%$) we readily see stimulated echo effects, unless we take the additional step of using crusher gradients before and after each π pulse with *a wide range of amplitudes or pulse directions*. When we do this, however, we eliminate signals from all of the spurious pathways, and in that case signal loss from finite duty cycle and rf inhomogeneity are the same for UDD, CPMG, and anti-UDD. Scalar couplings and diffusion effects are easily shown to be least important when the spacing is equal, as in CPMG. Thus nonidealities cannot explain the very substantial differences we see in tissue between these sequences.

However, this analysis suggests some serious difficulties with the quantum computing applications, which do not appear to have appreciated. The treatment of finite pulse duration in papers to date (simply replacing a binary $y(t)$ function with a ramped rise and fall) is vastly oversimplified because during the transition period, the coherence is partially transferred into population. A similar problem arises in treating Rabi frequency inhomogeneity, which generates small effects for any single pulse in the experimental demonstration in Ref. 8 but is extremely important when 500π pulses are given (as in that paper). More generally, a multiple echo sequence works much better for the coherence component in phase with the pulses than for the component out of phase (in NMR, this is the difference between the original sequence by Carr and Purcell[6] and the later modification by Meiboom and Gill[7]). In the former case, effects of rf inhomogeneity provides an immediately obvious modulation of the signal. Preservation of a qubit certainly requires preservation of more than one component of the magnetization—otherwise, the best sequence by far would simply be $(\pi/2)_x - T - (\pi/2)_{-x}$, preserving the coherence by storing it as population and recalling a stimulated echo. So the CPMG sequence vastly underestimates the error in coherence preservation, by observing only the well compensated component. Practical solutions for saving the other component (not critical for our work here, but important in iMQC applications as well as quantum computing) will at least require clever modulation of the echo pulse phases, as done in Ref. 15, and will probably require composite[17] or shaped adiabatic pulses.[18]

V. CONCLUSIONS

We have shown that a nonintuitive, unequal spacing of pulses in a multiple echo sequence, as derived theoretically by Uhrig for decoherence reduction in quantum computing, gives improved refocusing for some tissue types and also tends to suppress the (usually uninteresting) free water signals. We have not proven that the UDD sequence is a global optimum for MRI. In fact, different tissue types, with different spectral densities of the field fluctuations, will likely have different optimum solutions, and some further optimizations have already been done for the trapped-ion case.[8,26] However, the surprising result is that CPMG is clearly far from the optimum. As noted in Sec. I, there are many NMR applications for such sequences (including restricted diffusion, diffusion within internal structured gradients, and imaging in highly inhomogeneous fields). Contrast enhancement, reduced rf power dissipation for equivalent rephasing, and spectral density characterization are important in all of these applications, particularly as other obvious directions for further improvements are explored (e.g., phase shifts in the individual pulses, corrections for finite pulse widths, and shaped rf pulses). In addition, providing a new source of contrast (different from T_1 and T_2) which should correlate with tissue structure, and which does not require injected contrast agents, could dramatically impact standard practice for MRI of patients, particularly at lower fields where power dissipation is not an issue. Extensions to other pulsed coherent spectroscopies are feasible when multiple π pulses are possible (electron spin resonance and atomic spectroscopy). Finally, while we have focused here on dephasing, predicted extensions in the quantum computing literature to T_1 lifetime improvements[21] might also be of value for T_1-weighted images.

ACKNOWLEDGMENTS

This work was supported by NIH under Grant No. EB 02122.

[1] A. Ekert and R. Jozsa, Rev. Mod. Phys. **68**, 733 (1996); P. Shor, *Proceedings of the 35th Annual Symposium on Foundations of Computer Science* (IEEE Computer Society, New York, 1994).
[2] N. A. Gershenfeld and I. L. Chuang, Science **275**, 350 (1997).
[3] W. S. Warren, Science **277**, 1688 (1997); AIP Conf. Proc. **864**, 324 (2006).
[4] L. M. K. Vandersypen, M. Steffen, G. Bretya, C. S. Yannoni, M. H. Sherwood, and I. L. Chuang, Nature (London) **414**, 883 (2001).
[5] G. S. Uhrig, Phys. Rev. Lett. **98**, 100504 (2007).
[6] H. Y. Carr and E. M. Purcell, Phys. Rev. **94**, 630 (1954).
[7] S. Meiboom and D. Gill, Rev. Sci. Instrum. **29**, 688 (1958).
[8] M. J. Biercuk, H. Uys, A. P. VanDevender, N. Shiga, W. M. Itano, and J. J. Bollinger, Nature (London) **458**, 996 (2009).
[9] S. I. Doronin, A. V. Fedorova, E. B. Fel'dman, and A. I. Zenchuk, J. Chem. Phys. **131**, 104109 (2009).
[10] E. Ozarslan, N. Shemesh, and P. J. Basser, J. Chem. Phys. **130**, 104702 (2009).
[11] D. Frezzato, G. Kothe, and G. J. Moro, J. Chem. Phys. **119**, 6946 (2003).
[12] Y. Q. Song, S. Ryu, and P. N. Sen, Nature (London) **406**, 178 (2000).
[13] E. E. Sigmund, H. Cho, and Y. Q. Song, NMR Biomed. **22**, 436 (2009); E. Lammentausta, T. S. Silvast, J. Narvainen, J. S. Jurvelin, M. T. Nieminen, and O. H. Grohn, Phys. Med. Biol. **53**, 543 (2008).
[14] M. Klein, R. Fechete, D. E. Demco, and B. Blümich, J. Magn. Reson. **164**, 310 (2003); D. G. Rata, F. Casanova, J. Perlo, D. E. Demco, and B. Blümich, *ibid.* **180**, 229 (2006).

[15] U. Haeberlen, *High Resolution NMR in Solids: Selective Averaging* (Academic, New York, 1976).
[16] E. L. Hahn, Phys. Rev. **80**, 580 (1950).
[17] M. D. Hurlimann, J. Magn. Reson. **152**, 109 (2001).
[18] S. Michaeli, H. Gröhn, O. Gröhn, D. J. Sorce, R. Kauppinen, C. S. Springer, K. Ugurbil, and M. Garwood, Magn. Reson. Med. **53**, 823 (2005).
[19] B. Lee, W. M. Witzel, and S. Das Sarma, Phys. Rev. Lett. **100**, 160505 (2008).
[20] W. Yang and R. B. Liu, Phys. Rev. Lett. **101**, 180403 (2008).
[21] G. S. Uhrig, Phys. Rev. Lett. **102**, 120502 (2009).
[22] G. Galiana, R. T. Branca, E. R. Jenista, and W. S. Warren, Science **322**, 421 (2008); W. S. Warren, S. Ahn, M. Mescher, M. Garwood, K. Ugurbil, W. Richter, R. R. Rizi, J. Hopkins, and J. S. Leigh, *ibid.* **281**, 247 (1998).
[23] M. Carravetta, O. G. Johannessen, and M. H. Levitt, Phys. Rev. Lett. **92**, 153003 (2004).
[24] W. S. Warren, E. R. Jenista, R. T. Branca, and X. Chen, Science **323**, 1711 (2009).
[25] Y. Q. Song, J. Magn. Reson. **157**, 82 (2002).
[26] H. Uys, M. J. Biercuk, and J. J. Bollinger, Phys. Rev. Lett. **103**, 040501 (2009).